

Strong decays of the $1P$ and $2D$ doubly charmed states

Li-Ye Xiao,^{1,2,*} Qi-Fang Lü,^{3,4,†} and Shi-Lin Zhu^{1,2,5,‡}

¹*School of Physics and State Key Laboratory of Nuclear Physics and Technology, Peking University, Beijing 100871, China*

²*Center of High Energy Physics, Peking University, Beijing 100871, China*

³*Department of Physics, Hunan Normal University, and Key Laboratory of Low-Dimensional Quantum Structures and Quantum Control of Ministry of Education, Changsha 410081, China*

⁴*Synergetic Innovation Center for Quantum Effects and Applications (SICQEA), Hunan Normal University, Changsha 410081, China*

⁵*Collaborative Innovation Center of Quantum Matter, Beijing 100871, China*



(Received 26 December 2017; published 3 April 2018)

We perform a systematical investigation of the strong decay properties of the low-lying $1P$ - and $2D$ -wave doubly charmed baryons with the 3P_0 quark pair creation model. The main predictions include: (i) in the Ξ_{cc} and Ω_{cc} family, the $1P$ ρ mode excitations with $J^P = 1/2^-$ and $3/2^-$ should be the fairly narrow states, while, for the $1P$ λ mode excitations, they are most likely to be moderate states with a width of $\Gamma \sim 100$ MeV. (ii) The $2D_{\rho\rho}$ states mainly decay via emitting a heavy-light meson and the decay widths can reach several tens MeV if their masses are above the threshold of $\Lambda_c D$ or $\Xi_c D$, respectively. The $2D_{\lambda\lambda}$ states may be broad states with a width of $\Gamma > 100$ MeV.

DOI: [10.1103/PhysRevD.97.074005](https://doi.org/10.1103/PhysRevD.97.074005)

I. INTRODUCTION

Fifteen years ago, the SELEX Collaboration announced a doubly charmed baryon Ξ_{cc}^+ with mass 3519 ± 1 MeV [1]. One year later, another doubly charmed baryon Ξ_{cc}^{++} was reported at 3770 MeV by the same collaboration [2]. Unfortunately, those two signals $\Xi_{cc}^+(3519)$ and $\Xi_{cc}^{++}(3770)$ were not confirmed by other collaborations. Recently, the LHCb Collaboration discovered a doubly charmed baryon $\Xi_{cc}^{++}(3621)$ in the $\Lambda_c^+ K^- \pi^+ \pi^+$ mass spectrum [3]. Its mass was measured to be $3621.40 \pm 0.72 \pm 0.27 \pm 0.14$ MeV. The newly observed $\Xi_{cc}^{++}(3621)$ may provide an access point for the study of doubly heavy baryons and has attracted significant attention from the hadron physics community [4–19].

In the past twenty years, the properties of the doubly heavy baryons were extensively explored with various theoretical methods and models including the mass spectra [20–30] and semileptonic decays [6,31–42]. However, only a few discussions on the decay behavior

exist in literature [17–19,43–45]. In our previous work [17], we first systematically investigated the both strong and radiative transitions of the low-lying $1P$ -wave doubly heavy baryons with chiral and constituent quark model. In this work, we shall perform a systematic analysis of the two-body Okubo-Zweig-Iizuka (OZI) allowed strong decays of the $1P$ and $2D$ doubly charmed states with the quark pair creation (QPC) model, which may provide more information of their inner structures. The quark model classification, predicted masses [20], and OZI allowed decay modes [46] are summarized in Table I.

For the low-lying $1P$ and $2D$ doubly charmed baryons, their masses are large enough to allow the decay channels containing a heavy-light flavor meson. Thus, it is suitable to apply the QPC strong decay model. Meanwhile, for further understanding the strong decays of the doubly charmed baryons, it is necessary to make a comparison of the theoretical predictions with QPC model to the results with the chiral quark model [17].

The QPC strong decay model as a phenomenological method has been employed successfully in the description of the hadronic decays of the mesons [47–50] and singly charmed baryons [51–55]. Systematical study of the low-lying $1P$ and $2D$ doubly charmed states with the QPC model has not been performed yet. In the framework of the QPC model, we find that (i) our results of the decay patterns of the $1P$ states are highly comparable with those in our previous

*lyxiao@pku.edu.cn

†lvqifang@hunnu.edu.cn

‡zhushl@pku.edu.cn

Published by the American Physical Society under the terms of the [Creative Commons Attribution 4.0 International license](https://creativecommons.org/licenses/by/4.0/). Further distribution of this work must maintain attribution to the author(s) and the published article's title, journal citation, and DOI. Funded by SCOAP³.

TABLE I. Masses and possible two body strong decay channels of the $1P$ and $2D$ doubly charmed baryons (denoted by $|N^{2S+1}L_\sigma J^P\rangle$), where $|N^{2S+1}L_\sigma J^P\rangle = \sum_{L_z+S_z=J_z} \langle LL_z, SS_z | JJ_z \rangle^N \Psi_{LL_z}^\sigma \chi_{S_z} \phi$ [46]. The masses (MeV) are taken from the relativistic quark model [20].

State		Ξ_{cc}		Ω_{cc}	
$N^{2S+1}L_\sigma J^P$	Wave function	Mass [20]	Strong decay channel	Mass [20]	Strong decay channel
$ 0^2S_{\frac{1}{2}}^+\rangle$	${}^0\Psi_{00}^S \chi_{S_z}^\lambda \phi$	3620	...	3778	...
$ 0^4S_{\frac{3}{2}}^+\rangle$	${}^0\Psi_{00}^S \chi_{S_z}^s \phi$	3727	...	3872	...
$ 1^2P_{\rho\frac{1}{2}}^-\rangle$	${}^1\Psi_{1L_z}^\rho \chi_{S_z}^\rho \phi$	3838	...	4002	...
$ 1^2P_{\rho\frac{3}{2}}^-\rangle$		3959	...	4102	...
$ 1^2P_{\lambda\frac{1}{2}}^-\rangle$	${}^1\Psi_{1L_z}^\lambda \chi_{S_z}^\lambda \phi$	4136	$\Xi_{cc}^{(*)} \pi$	4271	$\Xi_{cc}^{(*)} K$
$ 1^2P_{\lambda\frac{3}{2}}^-\rangle$		4196	$\Xi_{cc}^{(*)} \pi$	4325	$\Xi_{cc}^{(*)} K$
$ 1^4P_{\lambda\frac{1}{2}}^-\rangle$	${}^1\Psi_{1L_z}^\lambda \chi_{S_z}^s \phi$	4053	$\Xi_{cc}^{(*)} \pi$	4208	$\Xi_{cc} K$
$ 1^4P_{\lambda\frac{3}{2}}^-\rangle$		4101	$\Xi_{cc}^{(*)} \pi$	4252	$\Xi_{cc}^{(*)} K$
$ 1^4P_{\lambda\frac{5}{2}}^-\rangle$		4155	$\Xi_{cc}^{(*)} \pi$	4303	$\Xi_{cc}^{(*)} K$
$ 2^2D_{\rho\rho\frac{3}{2}}^+\rangle$	${}^2\Psi_{2L_z}^{\rho\rho} \chi_{S_z}^\lambda \phi$		$\Lambda_c D$		$\Xi_c D$
$ 2^2D_{\rho\rho\frac{5}{2}}^+\rangle$			$\Lambda_c D, \Sigma_c^{(*)} D$		$\Xi_c D, \Xi_c^{\prime(*)} D$
$ 2^4D_{\rho\rho\frac{1}{2}}^+\rangle$	${}^2\Psi_{2L_z}^{\rho\rho} \chi_{S_z}^s \phi$		$\Lambda_c D$		$\Xi_c D$
$ 2^4D_{\rho\rho\frac{3}{2}}^+\rangle$			$\Lambda_c D, \Sigma_c D$		$\Xi_c D, \Xi_c' D$
$ 2^4D_{\rho\rho\frac{5}{2}}^+\rangle$			$\Lambda_c D, \Sigma_c^{(*)} D$		$\Xi_c D, \Xi_c^* D$
$ 2^4D_{\rho\rho\frac{7}{2}}^+\rangle$			$\Lambda_c D, \Sigma_c^{(*)} D, \Xi_c D_s, \Xi_c' D_s$		$\Xi_c D, \Xi_c^{(*)} D, \Omega_c^{(*)} D_s$
$ 2^2D_{\lambda\lambda\frac{3}{2}}^+\rangle$	${}^2\Psi_{2L_z}^{\lambda\lambda} \chi_{S_z}^\lambda \phi$		$\Xi_{cc}^{(*)} \pi, \Omega_{cc}^{(*)} K, \Lambda_c D, \Sigma_c^{(*)} D, \Xi_c D_s, \Xi_c^{\prime(*)} D_s$		$\Xi_{cc}^{(*)} K, \Omega_{cc}^{(*)} \eta, \Xi_c D, \Xi_c^{\prime(*)} D, \Omega_c^{(*)} D_s, \Omega_{cc}^{(*)} \eta'$
$ 2^2D_{\lambda\lambda\frac{5}{2}}^+\rangle$			$\Xi_{cc}^{(*)} \pi, \Omega_{cc}^{(*)} K, \Lambda_c D, \Sigma_c^{(*)} D, \Xi_c D_s, \Xi_c^{\prime(*)} D_s$		$\Xi_{cc}^{(*)} K, \Omega_{cc}^{(*)} \eta, \Xi_c D, \Xi_c^{\prime(*)} D, \Omega_c^{(*)} D_s, \Omega_{cc}^{(*)} \eta'$
$ 2^4D_{\lambda\lambda\frac{1}{2}}^+\rangle$	${}^2\Psi_{2L_z}^{\lambda\lambda} \chi_{S_z}^s \phi$		$\Xi_{cc}^{(*)} \pi, \Omega_{cc}^{(*)} K, \Lambda_c D, \Sigma_c^{(*)} D, \Xi_c D_s, \Xi_c' D_s$		$\Xi_{cc}^{(*)} K, \Omega_{cc}^{(*)} \eta, \Xi_c D, \Xi_c^{\prime(*)} D, \Omega_c D_s$
$ 2^4D_{\lambda\lambda\frac{3}{2}}^+\rangle$			$\Xi_{cc}^{(*)} \pi, \Omega_{cc}^{(*)} K, \Lambda_c D, \Sigma_c^{(*)} D, \Xi_c D_s, \Xi_c^{\prime(*)} D_s$		$\Xi_{cc}^{(*)} K, \Omega_{cc}^{(*)} \eta, \Omega_{cc} \eta', \Xi_c D, \Xi_c^{\prime(*)} D, \Omega_c^{(*)} D_s$
$ 2^4D_{\lambda\lambda\frac{5}{2}}^+\rangle$			$\Xi_{cc}^{(*)} \pi, \Omega_{cc}^{(*)} K, \Lambda_c D, \Sigma_c^{(*)} D, \Xi_c D_s, \Xi_c^{\prime(*)} D_s$		$\Xi_{cc}^{(*)} K, \Omega_{cc}^{(*)} \eta, \Omega_{cc} \eta', \Xi_c D, \Xi_c^{\prime(*)} D, \Omega_c^{(*)} D_s$
$ 2^4D_{\lambda\lambda\frac{7}{2}}^+\rangle$			$\Xi_{cc}^{(*)} \pi, \Omega_{cc}^{(*)} K, \Lambda_c D, \Sigma_c^{(*)} D, \Xi_c D_s, \Xi_c^{\prime(*)} D_s$		$\Xi_{cc}^{(*)} K, \Omega_{cc}^{(*)} \eta, \Omega_{cc} \eta', \Xi_c D, \Xi_c^{\prime(*)} D, \Omega_c^{(*)} D_s$

work [17]; (ii) the $2D_{\rho\rho}$ states mainly decay via emitting a heavy-light meson if their masses are above the threshold of $\Lambda_c D$ or $\Xi_c D$, respectively; (iii) although the $2D_{\lambda\lambda}$ states may be broad states with a width of $\Gamma > 100$ MeV, they still have the opportunity to be discovered via their main decay channels in future experiments.

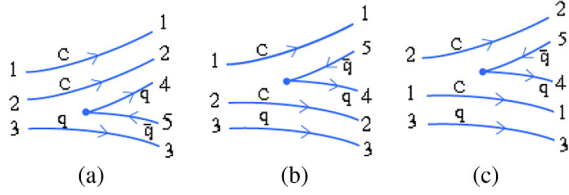
This paper is structured as follows. In Sec. II we give a brief review of the QPC model. We present our numerical results and discussions in Sec. III and summarize our results in Sec. IV.

II. 3P_0 MODEL

The QPC model was first proposed by Micu [56], Carlitz and Kislinger [57], and further developed by the Orsay group [58–60]. For the OZI-allowed strong decays of hadrons, this model assumes that a pair of quark $q\bar{q}$ is

created from the vacuum and then regroups with the quarks from the initial hadron to produce two outgoing hadrons. The created quark pair $q\bar{q}$ shall carry the quantum number of 0^{++} and be in a 3P_0 state. Thus the QPC model is also known as the 3P_0 model. This model has been extensively employed to study the OZI-allowed strong transitions of hadron systems. Here, we adopt this model to study the strong decays of the ccq system.

According to the quark rearrangement process, any of the three quarks in the initial baryon can go into the final meson. Thus three possible decay processes are taken into account as shown in Fig. 1. Now, we take the Fig. 1(a) decay process A (the initial baryon) $\rightarrow B$ (the final baryon) + C (the final meson) as an example to show how to calculate the decay width. In the nonrelativistic limit, the transition operator under the 3P_0 model is given by


 FIG. 1. Doubly charmed baryons decay process in the 3P_0 model.

$$T = -3\gamma \sum_m \langle 1m; 1-m|00 \rangle \int d^3\mathbf{p}_4 d^3\mathbf{p}_5 \delta^3(\mathbf{p}_4 + \mathbf{p}_5) \times \omega_0^{45} \varphi_0^{45} \chi_{1,-m}^{45} \mathcal{Y}_1^m \left(\frac{\mathbf{p}_4 - \mathbf{p}_5}{2} \right) a_{4i}^\dagger b_{5j}^\dagger, \quad (1)$$

where \mathbf{p}_i ($i = 4, 5$) represents the three-vector momentum of the i th quark in the created quark pair. $\omega_0^{45} = \delta_{ij}$ and $\varphi_0^{45} = (u\bar{u} + d\bar{d} + s\bar{s})/\sqrt{3}$ stand for the color singlet and flavor function, respectively. The solid harmonic polynomial $\mathcal{Y}_1^m(\mathbf{p}) \equiv |\mathbf{p}| Y_1^m(\theta_p, \phi_p)$ corresponds to the momentum-space distribution, and $\chi_{1,-m}^{45}$ is the spin triplet state for the created quark pair. The creation operator $a_{4i}^\dagger b_{5j}^\dagger$ denotes the quark pair-creation in the vacuum. The pair-creation strength γ is a dimensionless parameter, which is usually fixed by fitting the well measured partial decay widths.

According to the definition of the mock state [61], the spacial wave functions of the baryon and meson read, respectively,

$$\begin{aligned} & |A(N_A^{2S_A+1} L_A J_A M_{J_A})(\mathbf{p}_A) \rangle \\ &= \sqrt{2E_A} \varphi_A^{123} \omega_A^{123} \sum_{M_{L_A}, M_{S_A}} \langle L_A M_{L_A}; S_A M_{S_A} | J_A M_{J_A} \rangle \\ &\times \int d^3\mathbf{p}_1 d^3\mathbf{p}_2 d^3\mathbf{p}_3 \delta^3(\mathbf{p}_1 + \mathbf{p}_2 + \mathbf{p}_3 - \mathbf{p}_A) \\ &\times \Psi_{N_A L_A M_{L_A}(\mathbf{p}_1, \mathbf{p}_2, \mathbf{p}_3)} \chi_{S_A M_{S_A}}^{123} |q_1(\mathbf{p}_1) q_2(\mathbf{p}_2) q_3(\mathbf{p}_3) \rangle, \quad (2) \end{aligned}$$

$$\begin{aligned} & |C(N_C^{2S_C+1} L_C J_C M_{J_C})(\mathbf{p}_C) \rangle \\ &= \sqrt{2E_C} \varphi_C^{ab} \omega_C^{ab} \sum_{M_{L_C}, M_{S_C}} \langle L_C M_{L_C}; S_C M_{S_C} | J_C M_{J_C} \rangle \\ &\times \int d^3\mathbf{p}_a d^3\mathbf{p}_b \delta^3(\mathbf{p}_a + \mathbf{p}_b - \mathbf{p}_C) \\ &\times \Psi_{N_C L_C M_{L_C}(\mathbf{p}_a, \mathbf{p}_b)} \chi_{S_C M_{S_C}}^{ab} |q_a(\mathbf{p}_a) q_b(\mathbf{p}_b) \rangle. \quad (3) \end{aligned}$$

The \mathbf{p}_i ($i = 1, 2, 3$ and a, b) denotes the momentum of quarks in hadron A and C . $P_A(P_C)$ are the momentum of the hadron $A(C)$ and $\Psi_{N_A L_A M_{L_A}}(\Psi_{N_C L_C M_{L_C}})$ represent the space-wave functions. The 3P_0 model gives a good description of the decay properties of many observed mesons with the simple harmonic oscillator space-wave functions, which are adopted to describe the spatial wave function of both baryons and mesons in the present work. The spatial wave function of a baryon without the radial excitation is

$$\psi_{lm}^0(\mathbf{p}) = (-i)^l \left[\frac{2^{l+2}}{\sqrt{\pi}(2l+1)!!} \right]^{\frac{1}{2}} \left(\frac{1}{\alpha} \right)^{l+\frac{3}{2}} \exp\left(-\frac{\mathbf{p}^2}{2\alpha^2}\right) \mathcal{Y}_l^m(\mathbf{p}). \quad (4)$$

The ground state spatial wave function of a meson is

$$\psi_{0,0} = \left(\frac{R^2}{\pi} \right)^{\frac{3}{4}} \exp\left(-\frac{R^2 \mathbf{p}_{ab}^2}{2}\right), \quad (5)$$

where the \mathbf{p}_{ab} stands for the relative momentum between the quark and antiquark in the meson. Then, we can obtain the partial decay amplitude in the center of mass frame,

$$\begin{aligned} & \mathcal{M}^{M_{J_A} M_{J_B} M_{J_C}}(A \rightarrow B + C) \\ &= \gamma \sqrt{8E_A E_B E_C} \prod_{A,B,C} \langle \chi_{S_B M_{S_B}}^{124} \chi_{S_C M_{S_C}}^{35} | \chi_{S_A M_{S_A}}^{123} \chi_{1-m}^{45} \rangle \\ &\times \langle \varphi_B^{124} \varphi_C^{35} | \varphi_A^{123} \varphi_0^{45} \rangle I_{M_{L_A}, M_{L_C}}^{M_{L_A}, m}(\mathbf{p}). \quad (6) \end{aligned}$$

Here, $I_{M_{L_B}, M_{L_C}}^{M_{L_A}, m}(\mathbf{p})$ stands the spatial integral and more detailed information is presented in the Appendix A and B. The $\prod_{A,B,C}$ denotes the Clebsch-Gorden coefficients for the quark pair, initial and final hadrons, which come from the couplings among the orbital, spin, and total angular momentum. Its expression reads

$$\begin{aligned} & \sum \langle L_B M_{L_B}; S_B M_{S_B} | J_B M_{J_B} \rangle \langle L_C M_{L_C}; S_C M_{S_C} | J_C M_{J_C} \rangle \\ &\times \langle L_A M_{L_A}; S_A M_{S_A} | J_A M_{J_A} \rangle \langle 1m; 1-m|00 \rangle \quad (7) \end{aligned}$$

Finally, the decay width $\Gamma[A \rightarrow BC]$ reads

$$\Gamma[A \rightarrow BC] = \pi^2 \frac{|\mathbf{p}|}{M_A^2 2J_A + 1} \sum_{M_{J_A}, M_{J_B}, M_{J_C}} |\mathcal{M}^{M_{J_A} M_{J_B} M_{J_C}}|^2. \quad (8)$$

In the equation, \mathbf{p} is the momentum of the daughter baryon in the center of mass frame of the parent baryon A

TABLE II. Masses (MeV) of the baryons and mesons in the decays [3,20,62].

State	Mass	State	Mass	State	Mass
$\Xi_{cc}^{++(+)}$	3621.00	Σ_c^{++}	2453.97	π^0	134.977
$\Xi_{cc}^{*++(+)}$	3727.00	Σ_c^{*++}	2518.41	π^+	139.570
Ω_{cc}^+	3778.00	Σ_c^+	2452.90	K^\pm	493.677
Ω_{cc}^{*+}	3872.00	Σ_c^{*+}	2517.50	η	547.862
Λ_c^+	2286.46	Ξ_c^+	2467.93	η'	957.780
Ω_c^0	2695.20	$\Xi_c'^+$	2575.70	D^0	1864.83
Ω_c^{*0}	2765.90	Ξ_c^{*+}	2645.90	D^+	1869.58
				D_s^+	1968.27

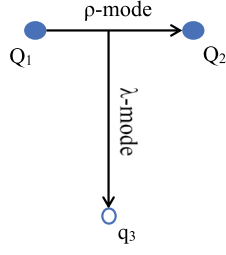


FIG. 2. The λ - and ρ - mode excitations of the ccq system where λ and ρ are the Jacobi coordinates defined as $\lambda = \frac{1}{\sqrt{6}}(\mathbf{r}_1 + \mathbf{r}_2 - 2\mathbf{r}_3)$ and $\rho = \frac{1}{\sqrt{2}}(\mathbf{r}_1 - \mathbf{r}_2)$, respectively. Q_1 and Q_2 stand for the charm quark, and q_3 stands for the light (u, d, s quark).

$$|\mathbf{p}| = \frac{\sqrt{[M_A^2 - (M_B - M_C)^2][M_A^2 - (M_B + M_C)^2]}}{2M_A} \quad (9)$$

In the present calculation, we adopt $m_u = m_d = 220$ MeV, $m_s = 419$ MeV, and $m_c = 1628$ MeV [49] for the constituent quark masses. The masses of the baryons and mesons involved in our calculations, listed in Table II, are from the Particle Data Group [62] except for the doubly charmed baryons, which is from Ref. [20]. The value of the harmonic oscillator strength R is 2.5 GeV^{-1} , for all light flavor mesons while it is $R = 1.67 \text{ GeV}^{-1}$ for the D meson and $R = 1.54 \text{ GeV}^{-1}$ for the D_s meson [49]. The parameter α_ρ of the ρ -mode excitation between the two charm quarks (see Fig. 2) is taken as $\alpha_\rho = 0.66 \text{ GeV}$ [17], while α_ρ between the two light quarks is taken as $\alpha_\rho = 0.4 \text{ GeV}$. Another harmonic oscillator parameter α_λ is obtained with the relation:

$$\alpha_\lambda = \left(\frac{3m_3}{2m_1 + m_3} \right)^{1/4} \alpha_\rho. \quad (10)$$

For the strength of the quark pair creation from the vacuum, we take the same value as in Ref. [49], $\gamma = 6.95$. For the strange quark pair $s\bar{s}$ creation, we use $\gamma_{s\bar{s}} = \gamma/\sqrt{3}$ [60].

III. CALCULATIONS AND RESULTS

For the P -wave doubly charmed states, the masses are adopted from Ref. [20] (showed in Table I) due to a good agreement with the mass of the lowest doubly charmed baryon $\Xi_{cc}^{++}(3621)$ observed by the LHCb collaboration. However, there is no prediction for the masses of the D -wave states. So the masses of the D -wave baryons are varied in a rough range when their decay properties are investigated.

A. The P -wave doubly charmed states

Within the quark model, there are two $1P_\rho$ doubly heavy baryons with $J^P = \frac{1}{2}^-$ and $J^P = \frac{3}{2}^-$, respectively. Their masses are above the threshold of $\Xi_{cc}\pi$ or $\Xi_{cc}K$. However,

the OZI-allowed two body strong decays are forbidden since the spatial wave functions for the $1P$ and $0S$ states are adopted with the simple harmonic oscillator wave functions which are orthogonal. In this work, we focus on the strong decays of the $1P_\lambda$ states.

We analyze the decay properties of the $1P_\lambda$ states in the Ξ_{cc} and Ω_{cc} family, and collect their partial strong decay widths in Table III. In the Ξ_{cc} family, the total decay width of $|\Xi_{cc}^2 P_{\lambda 2}^{1-}\rangle$ is about $\Gamma \sim 40 \text{ MeV}$, which is compatible with the result in Ref. [17]. The dominant decay modes are $\Xi_{cc}\pi$ and $\Xi_{cc}^*\pi$ with the partial decay ratio

$$\frac{\Gamma[|\Xi_{cc}^2 P_{\lambda 2}^{1-}\rangle \rightarrow \Xi_{cc}\pi]}{\Gamma[|\Xi_{cc}^2 P_{\lambda 2}^{1-}\rangle \rightarrow \Xi_{cc}^*\pi]} \simeq 1.18. \quad (11)$$

This value is about 2.5 times of the ratio in Ref. [17].

The states of $|\Xi_{cc}^2 P_{\lambda 2}^{3-}\rangle$ and $|\Xi_{cc}^4 P_{\lambda 2}^{3-}\rangle$ are most likely to be the moderate states with a width of $\Gamma \sim 130 \text{ MeV}$, and the $\Xi_{cc}^*\pi$ decay channel is their dominant decay mode. The partial decay width of $\Gamma[|\Xi_{cc}^2 P_{\lambda 2}^{3-}\rangle \rightarrow \Xi_{cc}\pi]$ is considerable. The partial decay width ratio is

$$\frac{\Gamma[|\Xi_{cc}^2 P_{\lambda 2}^{3-}\rangle \rightarrow \Xi_{cc}\pi]}{\Gamma[|\Xi_{cc}^2 P_{\lambda 2}^{3-}\rangle \rightarrow \Xi_{cc}^*\pi]} \simeq 0.18. \quad (12)$$

This ratio may be a useful distinction between $|\Xi_{cc}^2 P_{\lambda 2}^{3-}\rangle$ and $|\Xi_{cc}^4 P_{\lambda 2}^{3-}\rangle$ in future experiments. These results are in good agreement with the predictions in Ref. [17].

The state $|\Xi_{cc}^4 P_{\lambda 2}^{1-}\rangle$ has a broad width of $\Gamma \simeq 201 \text{ MeV}$, and the $\Xi_{cc}\pi$ decay channel almost saturates its total decay widths. This broad state may be observed in $\Xi_{cc}\pi$ channel in future experiments.

From the Table III, the state $|\Xi_{cc}^4 P_{\lambda 2}^{5-}\rangle$ may be a narrow state with a total decay width around $\Gamma \sim 60 \text{ MeV}$, which is about one half of that in Ref. [17]. This state decays mainly through the $\Xi_{cc}\pi$ channel. The predicted partial width ratio between $\Xi_{cc}\pi$ and $\Xi_{cc}^*\pi$ is

$$\frac{\Gamma[|\Xi_{cc}^4 P_{\lambda 2}^{5-}\rangle \rightarrow \Xi_{cc}\pi]}{\Gamma[|\Xi_{cc}^4 P_{\lambda 2}^{5-}\rangle \rightarrow \Xi_{cc}^*\pi]} \simeq 3.64, \quad (13)$$

which can be tested in future experiments.

In the Ω_{cc} family, the $|\Omega_{cc}^2 P_{\lambda 2}^{1-}\rangle$ and $|\Omega_{cc}^4 P_{\lambda 2}^{5-}\rangle$ might be two narrow states with a total decay width of $\Gamma \sim 40 \text{ MeV}$, and their strong decays are dominated by the $\Xi_{cc}K$ channel.

The decay width of the state $|\Omega_{cc}^4 P_{\lambda 2}^{1-}\rangle$ is about $\Gamma \sim 380 \text{ MeV}$. Meanwhile, its strong decays are governed by the $\Xi_{cc}K$ channel. In this case, the $|\Omega_{cc}^4 P_{\lambda 2}^{1-}\rangle$ might be too broad to be observed in experiments. However, for the states $|\Omega_{cc}^2 P_{\lambda 2}^{3-}\rangle$ and $|\Omega_{cc}^4 P_{\lambda 2}^{3-}\rangle$, if their masses lie below the threshold of Ξ_{cc}^*K , they are likely to be two fairly narrow states with the total decay widths of $\Gamma \sim 9 \text{ MeV}$ and $\Gamma \sim 2 \text{ MeV}$, respectively. Otherwise, they shall have a

TABLE III. The comparison of the partial decay widths of the $1P_\lambda$ states from the QPC model and the chiral quark model [17]. Γ_{total} stands for the total decay width and \mathcal{B} represent the ratio of the branching fractions $\Gamma[\Xi_{cc}\pi/K]/\Gamma[\Xi_{cc}^*\pi/K]$. The unit is MeV.

State	Mass	$\Gamma[\Xi_{cc}\pi]$		$\Gamma[\Xi_{cc}^*\pi]$		Total		\mathcal{B}	
		This work	Ref [17]	This work	Ref [17]	This work	Ref [17]	This work	Ref [17]
$ \Xi_{cc}^2 P_{\lambda 2}^{1-}\rangle$	4136	21.9	15.6	18.6	33.9	40.5	49.5	1.18	0.46
$ \Xi_{cc}^2 P_{\lambda 2}^{3-}\rangle$	4196	13.7	21.6	117	101	131	123	0.18	0.21
$ \Xi_{cc}^4 P_{\lambda 2}^{1-}\rangle$	4053	200	133	0.60	1.22	201	134	333	110
$ \Xi_{cc}^4 P_{\lambda 2}^{3-}\rangle$	4101	4.43	7.63	127	84.6	131	92.2	0.03	0.09
$ \Xi_{cc}^4 P_{\lambda 2}^{5-}\rangle$	4155	45.9	75.3	12.6	22.8	58.5	98.1	3.64	3.30

State	Mass	$\Gamma[\Xi_{cc}K]$		$\Gamma[\Xi_{cc}^*K]$		Total		\mathcal{B}	
		This work	Ref [17]	This work	Ref [17]	This work	Ref [17]	This work	Ref [17]
$ \Omega_{cc}^2 P_{\lambda 2}^{1-}\rangle$	4271	49.3	33.1	1.53	2.36	50.8	35.5	32.2	14.0
$ \Omega_{cc}^2 P_{\lambda 2}^{3-}\rangle$	4325	8.50	11.4	199	174	208	185	0.04	0.06
$ \Omega_{cc}^4 P_{\lambda 2}^{1-}\rangle$	4208	378	323	378	323
$ \Omega_{cc}^4 P_{\lambda 2}^{3-}\rangle$	4252	2.02	3.08	154	137	156	140	0.01	0.02
$ \Omega_{cc}^4 P_{\lambda 2}^{5-}\rangle$	4303	29.1	41.5	2.62	4.38	31.7	45.9	11.1	9.47

broad width of $\Gamma \sim 200$ MeV, and mainly decay into Ξ_{cc}^*K channel.

Considering the mass uncertainties of the $1P_\lambda$ states, we plot the strong decay width as a function of the mass in Figs. 3–4. From the Figs. 3–4, the partial width of dominant decay channel for most of states are sensitive to the mass. In addition, in the Ξ_{cc} family, if the $1P_\lambda$ states are above the threshold of $\Lambda_c D$, they can decay via $\Lambda_c D$ with a partial width about several MeV.

B. The D -wave doubly charmed states

1. ρ -mode excitations

Since we adopt the simple harmonic oscillator spatial wave functions in present work, the strong decays of $2D_{\rho\rho}$ doubly charmed states via emitting a light-flavor meson are forbidden due to the orthogonality of the spatial wave functions. So, we focus on the decay processes via emitting a heavy-light flavor meson. Due to the lack of the mass predictions for the D -wave doubly charmed states, we investigate the strong decay properties as the functions of the masses in a possible range.

First of all, we conduct systematic research on the strong decays of $2D_{\rho\rho}$ states in the Ξ_{cc} family in Fig. 5. For the state $|\Xi_{cc}^2 D_{\rho\rho 2}^{3+}\rangle$, we put the mass range between the $\Lambda_c D$ threshold ($M = 4152$ MeV) and $M = 4300$ MeV. From Fig. 5, we can see that the state $|\Xi_{cc}^2 D_{\rho\rho 2}^{3+}\rangle$ is a fairly narrow state with a width of a few MeV when its mass varies in the range. Its strong decay is dominated by $\Lambda_c D$.

Taking the masses of $|\Xi_{cc}^2 D_{\rho\rho 2}^{5+}\rangle$ and $|\Xi_{cc}^4 D_{\rho\rho 2}^{5+}\rangle$ in the range of (4.152–4.450) GeV, they are two narrow states

with a width of $\Gamma < 4$ MeV and mainly decay into $\Lambda_c D$ if their masses are below the threshold of $\Sigma_c^* D$. However, when the $\Sigma_c^* D$ channel is open, the total decay widths of those two states are sensitive to the mass and can increase up to several tenths MeV. If so, their dominant decay modes should be $\Sigma_c^* D$.

For the states $|\Xi_{cc}^4 D_{\rho\rho 2}^{1+}\rangle$ and $|\Xi_{cc}^4 D_{\rho\rho 2}^{3+}\rangle$, if their masses are above the threshold of $\Lambda_c D$, they mainly decay into $\Lambda_c D$ and have a width of several tens MeV.

Taking the mass of $|\Xi_{cc}^4 D_{\rho\rho 2}^{7+}\rangle$ in the range of (4.20–4.60) GeV, we get that the decay width of this state is about $\Gamma \simeq (0\text{--}120)$ MeV. Its strong decays are governed by the $\Lambda_c D$ channel in the whole mass region considered in the present work. When we take the mass of $|\Xi_{cc}^4 D_{\rho\rho 2}^{7+}\rangle$ with $M = 4373$ MeV, the predicted branching ratio is

$$\frac{\Gamma[\Lambda_c D]}{\Gamma_{\text{total}}} \simeq 98\%. \quad (14)$$

So, this state is most likely to be observed in the $\Lambda_c D$ channel.

Then, we analyze the decay properties of the $2D_{\rho\rho}$ states in the Ω_{cc} family, and plot the partial decay widths and total decay width as functions of the masses in Fig. 6.

To investigate the decay properties of the $|\Omega_{cc}^2 D_{\rho\rho 2}^{3+}\rangle$, we plot its decay widths as a function of the mass in the range of $M = (4.34\text{--}4.45)$ GeV. From the figure, its strong decay width is around a few MeV. This state mainly decays through the $\Xi_c D$ channel.

For the states $|\Omega_{cc}^2 D_{\rho\rho 2}^{5+}\rangle$ and $|\Omega_{cc}^4 D_{\rho\rho 2}^{5+}\rangle$, we take their masses in the range of $M = (4.34\text{--}4.60)$ GeV. If

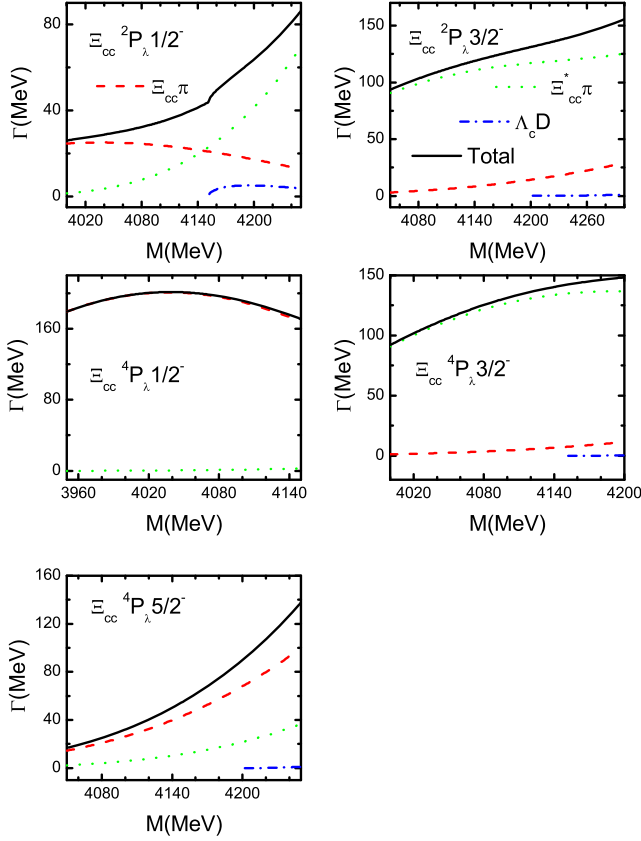


FIG. 3. The strong decay partial widths of the $1P_{\lambda}$ -wave Ξ_{cc} states as a function of the mass.

they lie below the Σ_c^*D threshold, the total decay widths are about $\Gamma < 3$ MeV, and are dominated by $\Xi_c D$. However, if their masses are above the threshold of Σ_c^*D , their dominant decay channels should be Σ_c^*D

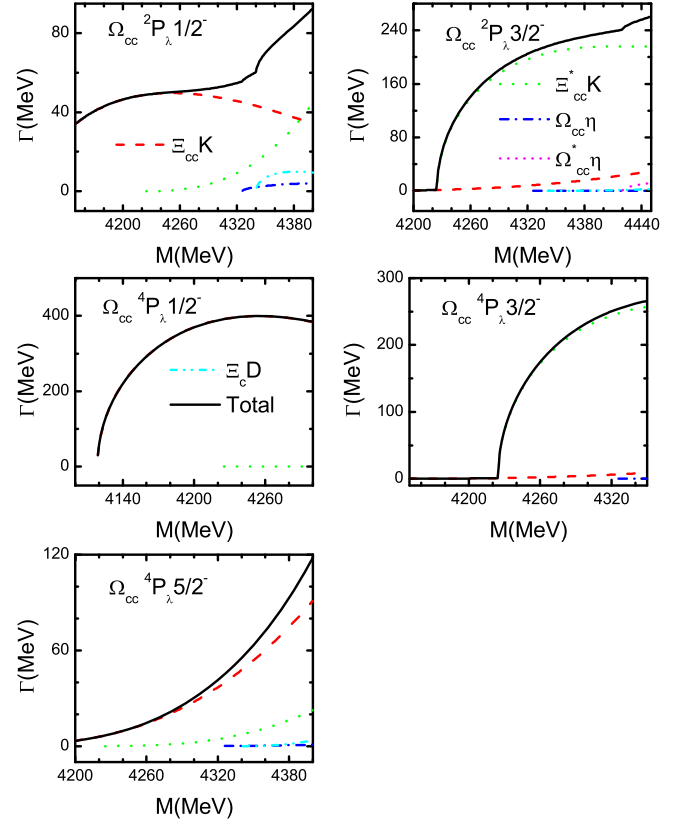


FIG. 4. The strong decay partial widths of the $1P_{\lambda}$ -wave Ω_{cc} states as a function of the mass.

and their total decay widths may reach several tenths MeV.

Taking the masses of $|\Omega_{cc}^4 D_{\rho\rho 2}^{1+}\rangle$ and $|\Omega_{cc}^4 D_{\rho\rho 2}^{3+}\rangle$ in the range of $M = (4.34-4.40)$ GeV and $M = (4.34-4.50)$ GeV,

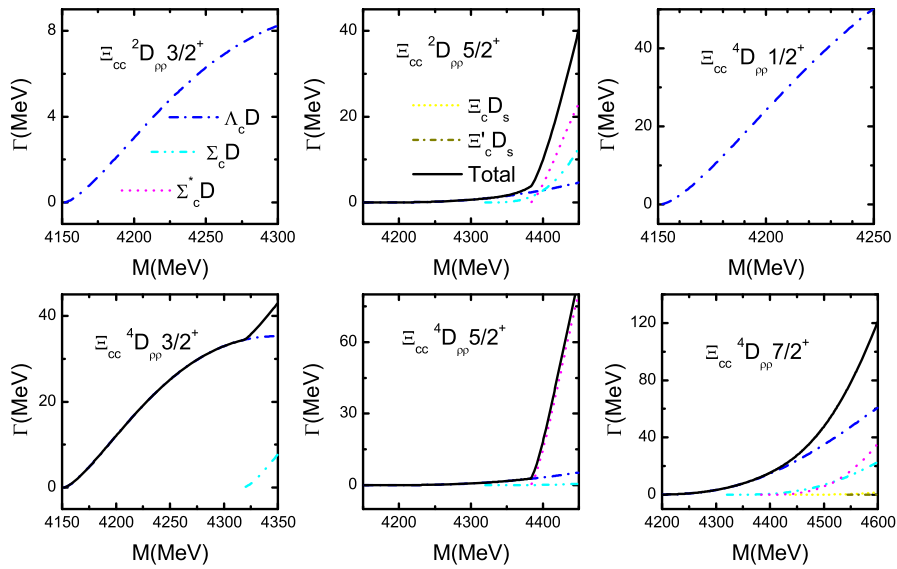
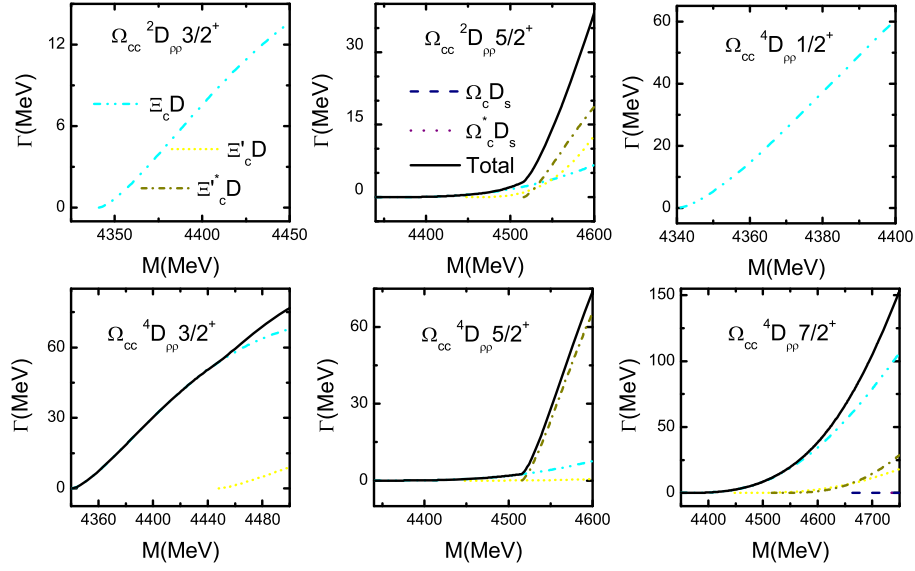


FIG. 5. The strong decay partial widths of the $2D_{\rho\rho}$ -wave Ξ_{cc} states as a function of the mass.


 FIG. 6. The strong decay partial widths of the $2D_{\rho\rho}$ -wave Ω_{cc} states as a function of the mass.

respectively, their decay widths depend considerably on their mass and are governed by the $\Xi_c D$ channel.

Assuming the mass of the $|\Omega_{cc} 4D_{\rho\rho} 7/2^+\rangle$ in the range of (4.35–4.75) GeV, this state has a width of $\Gamma \simeq (0\text{--}150)$ MeV. If we take the mass of $|\Omega_{cc} 4D_{\rho\rho} 7/2^+\rangle$ with $M = 4523$ MeV, the total decay width is about $\Gamma_{\text{total}} \simeq 12$ MeV, and the predicted branching ratio is

$$\frac{\Gamma[\Xi_c D]}{\Gamma_{\text{total}}} \simeq 98\%. \quad (15)$$

In brief, the $2D_{\rho\rho}$ states of Ξ_{cc} and Ω_{cc} can decay through emitting a heavy-light meson when their masses are above the threshold of $\Lambda_c D$ and $\Xi_c D$, respectively. Their total decay widths maybe reach several tens MeV if their masses are large enough. However, most of those states may lie below the threshold of $\Lambda_c D$ or $\Xi_c D$, respectively.

2. λ -mode excitations

As emphasized in our previous work [17], the λ -mode orbitally excited state has relatively larger mass than a ρ -mode orbitally excited state for the doubly charmed baryons. The $2D_{\lambda\lambda}$ states should be heavier than the $2D_{\rho\rho}$ states with the same J^P . Thus, many other decay modes are allowed when we study the strong decay properties of $2D_{\lambda\lambda}$ states.

In the Ξ_{cc} family, we estimate the mass of the $|\Xi_{cc} 2D_{\lambda\lambda} 3/2^+\rangle$ in the range of (4.50–4.90) GeV, and then investigate its strong decay properties as a function of the mass in Fig. 7. The decay width of the state $|\Xi_{cc} 2D_{\lambda\lambda} 3/2^+\rangle$ is about $\Gamma \simeq (100\text{--}650)$ MeV. The main decay channel is $\Xi_{cc}^* \pi$ and the predicted branching ratio is

$$\frac{\Gamma[\Xi_{cc}^* \pi]}{\Gamma_{\text{total}}} \simeq (77\text{--}87)\%. \quad (16)$$

On the other hand, the partial decay width of $\Gamma[|\Xi_{cc} 2D_{\lambda\lambda} 3/2^+\rangle \rightarrow \Sigma_c^* D]$ is sizable. The partial width ratio between $\Sigma_c^* D$ and $\Xi_{cc}^* \pi$ is

$$\frac{\Gamma[|\Xi_{cc} 2D_{\lambda\lambda} 3/2^+\rangle \rightarrow \Sigma_c^* D]}{\Gamma[|\Xi_{cc} 2D_{\lambda\lambda} 3/2^+\rangle \rightarrow \Xi_{cc}^* \pi]} \simeq 3.2\% \quad (17)$$

when we fix the mass of this state on $M = 4.70$ GeV.

For the state $|\Xi_{cc} 2D_{\lambda\lambda} 5/2^+\rangle$, its mass might be in the range of (4.55–4.95) GeV. The dependence of the strong decay properties of $|\Xi_{cc} 2D_{\lambda\lambda} 5/2^+\rangle$ on the mass is plotted in Fig. 7 as well. According to the figure, we can see that the state has a predicted width of $\Gamma \simeq (150\text{--}590)$ MeV, and mainly decays into $\Xi_{cc} \pi$ and $\Xi_{cc}^* \pi$. The predicted partial width ratio is

$$\frac{\Gamma[|\Xi_{cc} 2D_{\lambda\lambda} 5/2^+\rangle \rightarrow \Xi_{cc} \pi]}{\Gamma[|\Xi_{cc} 2D_{\lambda\lambda} 5/2^+\rangle \rightarrow \Xi_{cc}^* \pi]} \simeq (30\text{--}38)\%. \quad (18)$$

Meanwhile, the role of the $\Sigma_c D$ channel becomes more and more important as the mass increases. The branching ratio is

$$\frac{\Gamma[\Sigma_c D]}{\Gamma_{\text{total}}} \simeq (8\text{--}18)\%. \quad (19)$$

We estimate the mass of $|\Xi_{cc} 4D_{\lambda\lambda} 1/2^+\rangle$ in the range of (4.20–4.60) GeV and calculate its strong decay widths, which are shown in Fig. 7. From the figure, the state $|\Xi_{cc} 4D_{\lambda\lambda} 1/2^+\rangle$ is a moderate state with a width of $\Gamma \simeq (65\text{--}118)$ MeV, and its strong decays are governed by the $\Xi_{cc} \pi$ channel. The predicted branching ratio is

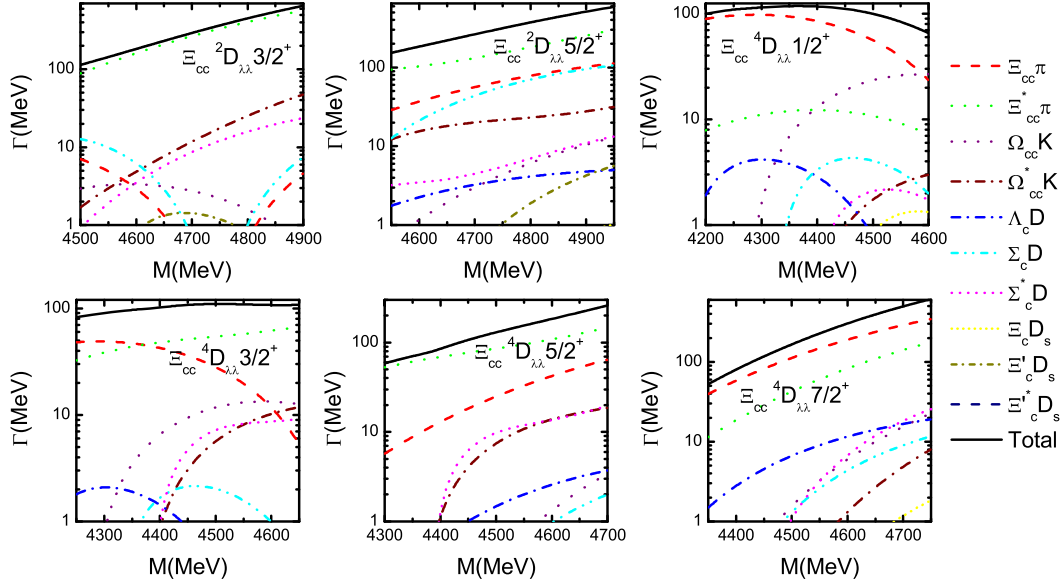


FIG. 7. The strong decay partial widths of the $2D_{\lambda\lambda}$ -wave Ξ_{cc} states as a function of the mass.

$$\frac{\Gamma[\Xi_{cc}\pi]}{\Gamma_{\text{total}}} \simeq (36\text{--}91)\%. \quad (20)$$

It should be pointed out that if the decay channel $\Omega_{cc}K$ is opened, which is sensitive to the mass, the branching ratio of this decay channel may reach 41%. Since the predicted width of $|\Xi_{cc}^4 D_{\lambda\lambda}^{1+}\rangle$ is not broad, this resonance might be observed in the $\Xi_{cc}\pi$ channel.

The mass of the state $|\Xi_{cc}^4 D_{\lambda\lambda}^{3+}\rangle$ might be in the range of (4.25–4.65) GeV, which is ~ 50 MeV heavier than that of the state $|\Xi_{cc}^4 D_{\lambda\lambda}^{1+}\rangle$. We plot the strong decay properties of $|\Xi_{cc}^4 D_{\lambda\lambda}^{3+}\rangle$ as a function of the mass in Fig. 7. The state $|\Xi_{cc}^4 D_{\lambda\lambda}^{3+}\rangle$ may be a moderate state with a width of $\Gamma \simeq (82\text{--}110)$ MeV, and its strong decays are dominated by the $\Xi_{cc}\pi$ and $\Xi_{cc}^*\pi$ channels. However, the partial width of $\Xi_{cc}\pi$ decreases dramatically with the mass. So, the predicted branching ratio of the $\Xi_{cc}\pi$ channel varies in a wide range of

$$\frac{\Gamma[\Xi_{cc}\pi]}{\Gamma_{\text{total}}} \simeq (58\text{--}5)\%. \quad (21)$$

The branching ratio of the $\Xi_{cc}^*\pi$ channel is stable, which is

$$\frac{\Gamma[\Xi_{cc}^*\pi]}{\Gamma_{\text{total}}} \simeq (39\text{--}62)\%. \quad (22)$$

This state has good potential to be discovered in the $\Xi_{cc}\pi$ and $\Xi_{cc}^*\pi$ channels.

For the state $|\Xi_{cc}^4 D_{\lambda\lambda}^{5+}\rangle$, we plot its partial decay widths and total widths as a function of the mass in the range of (4.30–4.70) GeV. From Fig. 7, its total decay width is about $\Gamma \simeq (59\text{--}260)$ MeV. The partial decay width ratio of the main two decay channels $\Xi_{cc}\pi$ and $\Xi_{cc}^*\pi$ is

$$\frac{\Gamma[|\Xi_{cc}^4 D_{\lambda\lambda}^{5+}\rangle \rightarrow \Xi_{cc}\pi]}{\Gamma[|\Xi_{cc}^4 D_{\lambda\lambda}^{5+}\rangle \rightarrow \Xi_{cc}^*\pi]} \simeq (11\text{--}44)\%. \quad (23)$$

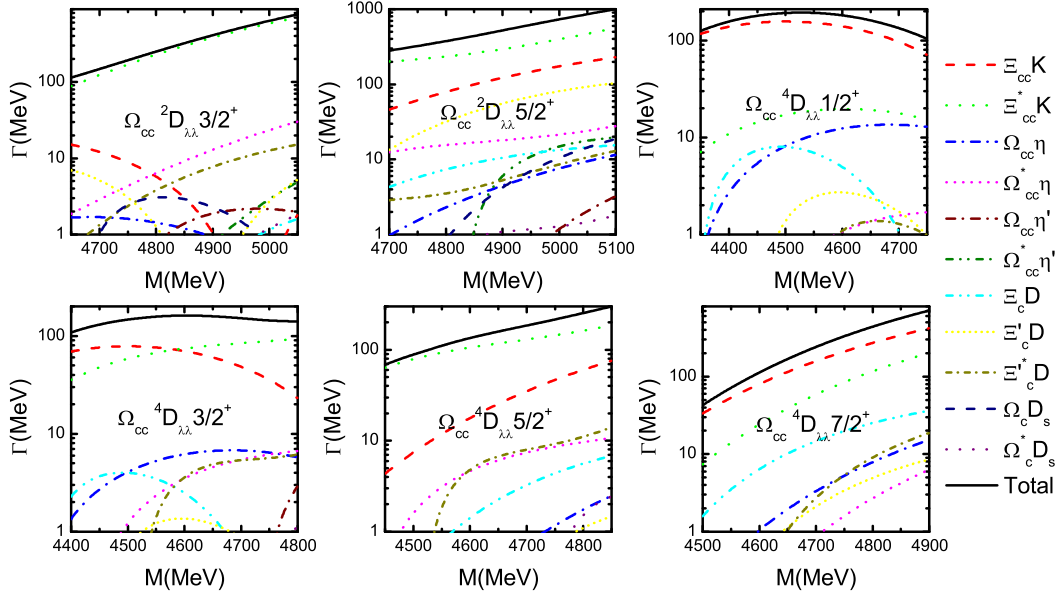
Meanwhile, from the Fig. 7 we notice that the strong decays of the state $|\Xi_{cc}^4 D_{\lambda\lambda}^{7+}\rangle$ are dominated by the $\Xi_{cc}\pi$ and $\Xi_{cc}^*\pi$ channels as well, when the mass lies in the range of (4.35–4.75) GeV. But the total decay width of $|\Xi_{cc}^4 D_{\lambda\lambda}^{7+}\rangle$ is about $\Gamma \simeq (52\text{--}610)$ MeV, which shows stronger dependency on the mass than that of $|\Xi_{cc}^4 D_{\lambda\lambda}^{5+}\rangle$, and the predicted ratio between $\Xi_{cc}\pi$ and $\Xi_{cc}^*\pi$ is

$$\frac{\Gamma[|\Xi_{cc}^4 D_{\lambda\lambda}^{7+}\rangle \rightarrow \Xi_{cc}\pi]}{\Gamma[|\Xi_{cc}^4 D_{\lambda\lambda}^{7+}\rangle \rightarrow \Xi_{cc}^*\pi]} \simeq (3.5\text{--}7.8). \quad (24)$$

In addition, we extract the strong decays of the $2D_{\lambda\lambda}$ states in the Ω_{cc} family, and plot their decay properties as functions of the masses in Fig. 8. Usually, the mass of the Ω_{cc} resonances is about 150 MeV larger than that of the Ξ_{cc} resonances [19,20]. Thus we estimate the mass of the state $|\Omega_{cc}^2 D_{\lambda\lambda}^{3+}\rangle$ might be in the range of (4.65–5.05) GeV. According to our theoretical calculations, $|\Omega_{cc}^2 D_{\lambda\lambda}^{3+}\rangle$ is a broad state with a width of $\Gamma \simeq (114\text{--}769)$ MeV, and Ξ_{cc}^*K almost saturates its total decay widths.

Meanwhile, the state $|\Omega_{cc}^2 D_{\lambda\lambda}^{5+}\rangle$ is most likely to be a very broad state as well, and the total decay width is about $\Gamma \simeq (280\text{--}1000)$ MeV with the mass in the range of (4.70–5.10) GeV. Its strong decays are governed by the $\Xi_{cc}K$ and Ξ_{cc}^*K channels. The predicted partial width ratio between $\Xi_{cc}K$ and Ξ_{cc}^*K is

$$\frac{\Gamma[|\Omega_{cc}^2 D_{\lambda\lambda}^{5+}\rangle \rightarrow \Xi_{cc}K]}{\Gamma[|\Omega_{cc}^2 D_{\lambda\lambda}^{5+}\rangle \rightarrow \Xi_{cc}^*K]} \simeq (23\text{--}41)\%. \quad (25)$$


 FIG. 8. The strong decay partial widths of the $2D_{\lambda\lambda}$ -wave Ω_{cc} states as a function of the mass.

The partial width of $\Xi'_{cc}D$ is sizable as well. This broad state might be hard to be observed in experiments.

Taking the mass of $|\Omega_{cc} 4D_{\lambda\lambda} 1^+\rangle$ in the range of (4.35–4.75) GeV, the state $|\Omega_{cc} 4D_{\lambda\lambda} 1^+\rangle$ might be a moderate state with a width of $\Gamma \simeq (104\text{--}194)$ MeV, and mainly decays into the $\Xi_{cc}K$ channel. Such a moderate state has some possibility to be observed in future experiments.

As to the state $|\Omega_{cc} 4D_{\lambda\lambda} 3^+\rangle$, we plot its strong decay properties as a function of the mass in the range of (4.40–4.80) GeV in Fig. 8. The total decay width of $|\Omega_{cc} 4D_{\lambda\lambda} 3^+\rangle$ is $\Gamma \simeq (108\text{--}161)$ MeV. Its strong decays are dominated by the $\Xi_{cc}K$ and Ξ_{cc}^*K channels, and the predicted partial decay width ratio is

$$\frac{\Gamma[|\Omega_{cc} 4D_{\lambda\lambda} 3^+\rangle \rightarrow \Xi_{cc}K]}{\Gamma[|\Omega_{cc} 4D_{\lambda\lambda} 3^+\rangle \rightarrow \Xi_{cc}^*K]} \simeq (1.95\text{--}0.24). \quad (26)$$

The total decay width of $|\Omega_{cc} 4D_{\lambda\lambda} 5^+\rangle$ is $\Gamma \simeq (68\text{--}300)$ MeV with the mass in the range of (4.45–4.85) GeV. From the Fig 8, this state mainly decays through the Ξ_{cc}^*K channel. The branching ratio is

$$\frac{\Gamma[\Xi_{cc}^*K]}{\Gamma_{\text{total}}} \simeq (93\text{--}62)\%. \quad (27)$$

The partial width of the $\Xi_{cc}K$ channel is sizable as well.

The partial decay widths of the $|\Omega_{cc} 4D_{\lambda\lambda} 7^+\rangle$ strongly depend on its mass. Taking the mass of $|\Omega_{cc} 4D_{\lambda\lambda} 7^+\rangle$ in the range of (4.50–4.90) GeV, the total decay width varies in a wide range of $\Gamma \simeq (43\text{--}708)$ MeV. Its strong decays are governed by the $\Xi_{cc}K$ and Ξ_{cc}^*K channels, and the partial decay width ratio is

$$\frac{\Gamma[|\Omega_{cc} 4D_{\lambda\lambda} 7^+\rangle \rightarrow \Xi_{cc}^*K]}{\Gamma[|\Omega_{cc} 4D_{\lambda\lambda} 7^+\rangle \rightarrow \Xi_{cc}K]} \simeq (22\text{--}48)\%. \quad (28)$$

Meanwhile, the partial decay width of $\Xi_c D$ is sizable, and the predicted partial width ratio between $\Xi_c D$ and $\Xi_{cc}K$ is

$$\frac{\Gamma[|\Omega_{cc} 4D_{\lambda\lambda} 7^+\rangle \rightarrow \Xi_c D]}{\Gamma[|\Omega_{cc} 4D_{\lambda\lambda} 7^+\rangle \rightarrow \Xi_{cc}K]} \simeq (4.7\text{--}8.6)\%. \quad (29)$$

In conclusion, in the Ξ_{cc} and Ω_{cc} family, the $2D_{\lambda\lambda}$ states with $J^P = 1/2^+, 7/2^+$ mainly decay into the ground state with $J^P = 3/2^+$ through emitting a light-flavor meson, while the $2D_{\lambda\lambda}$ states with $J^P = 3/2^+, 5/2^+$ mainly decay into the ground state with $J^P = 1/2^+$ plus a light-flavor meson. The states $4D_{\lambda\lambda} 1^+$ and $4D_{\lambda\lambda} 3^+$ are most likely to be the moderate states with the total widths of $\Gamma \sim 100$ MeV, which are insensitive to their masses, and might be discovered in their dominant decay channels.

It should be pointed out that all of the theoretical predictions of the strong decays for the low-lying $1P$ and $2D$ doubly charmed baryons are obtained with the fixed harmonic oscillator parameter $\alpha_\rho = 660$ MeV as in the charmonium system. However, the parameter α_ρ bares a large uncertainty. It is necessary to further consider the decay properties as a function of the parameter α_ρ . Our theoretical results show that the decay properties of the doubly charmed states we considered in the present work are not sensitive to this parameter when it varies within a appropriate range. On the other hand, the hadronic loop effects are not included in this calculations. There are some discussions about the meson-baryon loop effects in light baryons [63–66] and meson-meson loop effects in mesons [67–71]. However, it should be emphasized that hadronic

loop effects in heavy quarkonium are not obvious [67,68]. The main predictions in models without or with coupled-channel effects maybe have little different from each other, i.e., part of the hadronic loop effects can be absorbed into the model parameters. In the present work, we consider the doubly-charmed baryons(ccq) which also belong to the heavy quark system. So, the hadronic loop effects would be partly absorbed into the model parameters and don't change our main predictions. Moreover, due to many new parameters from the hadronic loop model and the lack of the experimental data, it is difficult to calculate the hadronic loop effects precisely in the doubly charmed baryon sector.

IV. SUMMARY

In the present work, we have systematically studied the strong decay properties of the low-lying $1P$ and $2D$ doubly charmed baryons in the framework of the 3P_0 quark pair creation model. Our main results are summarized as follows.

For the $1P$ ρ -mode doubly charmed baryons, their decay widths should be fairly narrow because of the absence of the strong decay modes. In addition, for the $1P$ λ -mode excitations, the states $|{}^2P_{\lambda_2}^{\frac{3}{2}-}\rangle$ and $|{}^4P_{\lambda_2}^{\frac{3}{2}-}\rangle$ are predicted to be moderate states with a width of $\Gamma \sim 150$ MeV. Their strong decays are governed by the $\Xi_{cc}^*\pi$ or Ξ_{cc}^*K channel. However, the states $|{}^2P_{\lambda_2}^{\frac{1}{2}-}\rangle$ and $|{}^4P_{\lambda_2}^{\frac{5}{2}-}\rangle$ are most likely to be narrow states with a total decay width of $\Gamma \sim 40$ MeV, and their strong decays are dominated by the $\Xi_{cc}\pi$ or $\Xi_{cc}K$ channel. Such narrow states have good potential to be observed in future experiments. Meanwhile, the dominant decay mode of the state $|{}^4P_{\lambda_2}^{\frac{1}{2}-}\rangle$ is $\Xi_{cc}\pi$ or $\Xi_{cc}K$ as well, but the total decay width of this state is about $\Gamma > 200$ MeV.

Since the strong decays of $2D_{\rho\rho}$ doubly charmed baryons via emitting a light-flavor meson are forbidden, they mainly decay via emitting a heavy-light meson with a total decay width of several tens MeV if their masses are large enough. The partial strong decay widths of the $2D_{\rho\rho}$ doubly charmed baryons strongly depend on their masses. The measurement of masses in the future will be helpful to understand their inner structures.

Within the range of mass we considered, the $2D_{\lambda\lambda}$ states with $J^P = 1/2^+, 7/2^+$ mainly decay through the $\Xi_{cc}^*\pi$ or Ξ_{cc}^*K channels, respectively, while the $2D_{\lambda\lambda}$ states with $J^P = 3/2^+, 5/2^+$ mainly decay through the $\Xi_{cc}\pi$ or $\Xi_{cc}K$ channels. It should be remarked that the states $|{}^4D_{\lambda\lambda}^{\frac{1}{2}+}\rangle$ and $|{}^4D_{\lambda\lambda}^{\frac{3}{2}+}\rangle$ are most likely to be discovered in their corresponding dominant decay channels because of their not broad widths of $\Gamma \sim 100$ MeV, which are insensitive to their masses.

ACKNOWLEDGMENTS

We would like to thank Xian-Hui Zhong for very helpful discussions. This work is supported by the National Natural

Science Foundation of China under Grants No. 11575008, No. 11705056, No. 11621131001 and 973 program. This work is also in part supported by China Postdoctoral Science Foundation under Grant No. 2017M620492.

APPENDIX A: THE DECAY MODE WITH DOUBLY CHARMED BARYON PLUS A LIGHT-FLAVOR MESON

The harmonic oscillator wave functions for the orbitally excited baryons in our calculation are

$$\begin{aligned} \psi(l_\rho, m_\rho, l_\lambda, m_\lambda) = & (-i)^l \left[\frac{2^{l_\rho+2}}{\sqrt{\pi}(2l_\rho+1)!!} \right]^{\frac{1}{2}} \left(\frac{1}{\alpha_\rho} \right)^{\frac{3}{2}+l_\rho} \mathcal{Y}_{l_\rho}^{m_\rho}(\mathbf{p}_\rho) \\ & \times (-i)^l \left(\frac{2^{l_\lambda+2}}{\sqrt{\pi}(2l_\lambda+1)!!} \right)^{\frac{1}{2}} \left(\frac{1}{\alpha_\lambda} \right)^{\frac{3}{2}+l_\lambda} \mathcal{Y}_{l_\lambda}^{m_\lambda}(\mathbf{p}_\lambda) \\ & \times \exp\left(-\frac{\mathbf{p}_\rho^2}{2\alpha_\rho^2} - \frac{\mathbf{p}_\lambda^2}{2\alpha_\lambda^2}\right), \end{aligned} \quad (\text{A1})$$

where $\mathbf{p}_\rho = \frac{1}{\sqrt{2}}(\mathbf{p}_1 - \mathbf{p}_2)$ and $\mathbf{p}_\lambda = \frac{1}{\sqrt{6}}(\mathbf{p}_1 + \mathbf{p}_2 - 2\mathbf{p}_3)$. The ground state wave function of the meson is

$$\psi(0, 0) = \left(\frac{R^2}{\pi} \right)^{\frac{3}{4}} \exp\left(-\frac{R^2 \mathbf{p}_{ab}^2}{2}\right), \quad (\text{A2})$$

where \mathbf{p}_{ab} stands for the relative momentum between the quark and antiquark in a meson.

Since all the final states are in the S -wave ground states in the present work, the momentum space integration $I_{M_{L_B}, M_{L_C}}^{M_{L_A}, m}(\mathbf{p})$ can be further expressed as $\Pi(l_{\rho A}, m_{\rho A}, l_{\lambda A}, m_{\lambda A}, m)$. Based on Fig. 1(a), the explicit form of the momentum space integration $\Pi(l_{\rho A}, m_{\rho A}, l_{\lambda A}, m_{\lambda A}, m)$ are presented in the following.

For the S -wave decay,

$$\Pi(0, 0, 0, 0, 0) = \beta |\mathbf{p}| \Delta_{0,0}. \quad (\text{A3})$$

For the P -wave decay,

$$\Pi(0, 0, 1, 0, 0) = \left(\frac{1}{\sqrt{6}\lambda_2} - \frac{\lambda_3}{2\lambda_2} \beta |\mathbf{p}|^2 \right) \Delta_{0,1}, \quad (\text{A4})$$

$$\begin{aligned} \Pi(0, 0, 1, 1, -1) &= -\frac{1}{\sqrt{6}\lambda_2} \Delta_{0,1} \\ &= \Pi(0, 0, 1, -1, 1). \end{aligned} \quad (\text{A5})$$

For the D -wave decay,

$$\Pi(0, 0, 2, 0, 0) = \left(\frac{\lambda_3^2}{2\lambda_2^2} \beta |\mathbf{p}|^3 - \frac{\sqrt{6}\lambda_3}{3\lambda_2^2} |\mathbf{p}| \right) \Delta_{0,2}, \quad (\text{A6})$$

$$\Pi(0, 0, 2, 1, -1) = \frac{\lambda_3}{\sqrt{2}\lambda_2^2} |\mathbf{p}| \Delta_{0,2} = \Pi(0, 0, 2, -1, 1). \quad (\text{A7})$$

Here,

$$\lambda_1 = \frac{1}{\alpha_\rho^2}, \quad \lambda_2 = \frac{1}{\alpha_\lambda^2} + \frac{R^2}{3}, \quad \lambda_3 = \frac{2}{\sqrt{6}\alpha_\lambda^2} + \frac{R^2}{\sqrt{6}}, \quad (\text{A8})$$

$$\lambda_4 = \frac{1}{3\alpha_\lambda^2} + \frac{R^2}{8}, \quad \beta = 1 - \frac{\lambda_3}{\sqrt{6}\lambda_2}, \quad (\text{A9})$$

for the above expressions and

$$\begin{aligned} \Delta_{0,0} &= \left(\frac{1}{\pi\alpha_\rho^2}\right)^{\frac{3}{4}} \left(\frac{1}{\pi\alpha_\lambda^2}\right)^{\frac{3}{4}} \left(\frac{R^2}{\pi}\right)^{\frac{3}{4}} \left(\frac{\pi^2}{\lambda_1\lambda_2}\right)^{\frac{3}{2}} \\ &\times \exp\left[-\left(\lambda_4 - \frac{\lambda_3^2}{4\lambda_2}\right)|\mathbf{p}|^2\right] \\ &\times \left(-\sqrt{\frac{3}{4\pi}}\right) \left(\frac{1}{\pi\alpha_\rho^2}\right)^{\frac{3}{4}} \left(\frac{1}{\pi\alpha_\lambda^2}\right)^{\frac{3}{4}}, \end{aligned} \quad (\text{A10})$$

$$\begin{aligned} \Delta_{0,1} &= \left(\frac{1}{\pi\alpha_\rho^2}\right)^{\frac{3}{4}} \left(\frac{1}{\pi\alpha_\lambda^2}\right)^{\frac{3}{4}} \left(\frac{R^2}{\pi}\right)^{\frac{3}{4}} \left(\frac{\pi^2}{\lambda_1\lambda_2}\right)^{\frac{3}{2}} \\ &\times \exp\left[-\left(\lambda_4 - \frac{\lambda_3^2}{4\lambda_2}\right)|\mathbf{p}|^2\right] \\ &\times \frac{3i}{4\pi} \left(\frac{1}{\pi\alpha_\rho^2}\right)^{\frac{3}{4}} \left(\frac{8}{3\sqrt{\pi}}\right)^{\frac{1}{2}} \left(\frac{1}{\alpha_\lambda^2}\right)^{\frac{5}{4}}, \end{aligned} \quad (\text{A11})$$

$$\begin{aligned} \Delta_{0,2} &= \left(\frac{1}{\pi\alpha_\rho^2}\right)^{\frac{3}{4}} \left(\frac{1}{\pi\alpha_\lambda^2}\right)^{\frac{3}{4}} \left(\frac{R^2}{\pi}\right)^{\frac{3}{4}} \left(\frac{\pi^2}{\lambda_1\lambda_2}\right)^{\frac{3}{2}} \\ &\times \exp\left[-\left(\lambda_4 - \frac{\lambda_3^2}{4\lambda_2}\right)|\mathbf{p}|^2\right] \\ &\times \frac{\sqrt{15}}{8\pi} \left(\frac{1}{\pi\alpha_\rho^2}\right)^{\frac{3}{4}} \left(\frac{16}{15\sqrt{\pi}}\right)^{\frac{1}{2}} \left(\frac{1}{\alpha_\lambda^2}\right)^{\frac{7}{4}}. \end{aligned} \quad (\text{A12})$$

APPENDIX B: THE DECAY MODE WITH A SINGLY HEAVY BARYON PLUS A HEAVY-LIGHT MESON

From Fig. 1(c), the momentum space integration $\Pi(l_{\rho A}, m_{\rho A}, l_{\lambda A}, m_{\lambda A}, m)$ can be expressed in the following.
For the S -wave decay,

$$\Pi(0, 0, 0, 0, 0) = \beta |\mathbf{p}| \Delta_{0,0}. \quad (\text{B1})$$

For the P -wave decay,

$$\Pi(0, 0, 1, 0, 0) = -\frac{1}{2f_1} (f_2 \beta |\mathbf{p}|^2 + \zeta) \Delta_{0,1}, \quad (\text{B2})$$

$$\Pi(0, 0, 1, 1, -1) = \Pi(0, 0, 1, -1, 1) = \frac{\zeta}{2f_1} \Delta_{0,1}, \quad (\text{B3})$$

$$\Pi(1, 0, 0, 0, 0) = \left(\beta \varpi |\mathbf{p}|^2 + \frac{1}{2\sqrt{2}\lambda_1} + \frac{\zeta\lambda_2}{4\lambda_1 f_1}\right) \Delta_{1,0}, \quad (\text{B4})$$

$$\begin{aligned} \Pi(1, 1, 0, 0, -1) &= -\left(\frac{\zeta\lambda_2}{4\lambda_1 f_1} + \frac{1}{2\sqrt{2}\lambda_1}\right) \Delta_{1,0} \\ &= \Pi(1, -1, 0, 0, 1). \end{aligned} \quad (\text{B5})$$

For the D -wave decay,

$$\Pi(0, 0, 2, 0, 0) = \frac{f_2}{f_1^2} \left(\frac{1}{2}\beta f_2 |\mathbf{p}|^3 + \zeta |\mathbf{p}|\right) \Delta_{0,2}, \quad (\text{B6})$$

$$\Pi(0, 0, 2, 1, -1) = -\frac{\sqrt{3}f_2}{2f_1^2} \zeta |\mathbf{p}| \Delta_{0,2} = \Pi(0, 0, 2, -1, 1), \quad (\text{B7})$$

$$\Pi(2, 0, 0, 0, 0) = 2 \left(\beta \varpi^2 |\mathbf{p}|^2 + \frac{\varpi}{\sqrt{2}\lambda_1} + \frac{\lambda_2 \zeta \varpi}{2\lambda_1 f_1}\right) |\mathbf{p}| \Delta_{2,0}, \quad (\text{B8})$$

$$\begin{aligned} \Pi(2, 1, 0, 0, -1) &= -\left(\frac{\sqrt{6}\varpi}{2\lambda_1} + \frac{\sqrt{3}\lambda_2 \varpi \zeta}{2\lambda_1 f_1}\right) |\mathbf{p}| \Delta_{2,0} \\ &= \Pi(2, -1, 0, 0, 1), \end{aligned} \quad (\text{B9})$$

$$\begin{aligned} \Pi(1, 0, 1, 0, 0) &= \left(\frac{f_2 \varpi \beta}{2f_1} |\mathbf{p}|^2 + \frac{\lambda_2 f_2 \zeta}{8\lambda_1 f_1^2} + \frac{\varpi \zeta}{2f_1} + \frac{\lambda_2 \beta}{4\lambda_1 f_1}\right. \\ &\quad \left. + \frac{\sqrt{2}f_2}{8\lambda_1 f_1}\right) |\mathbf{p}| \Delta_{1,1}, \end{aligned} \quad (\text{B10})$$

$$\Pi(1, 0, 1, 1, -1) = -\frac{\varpi \zeta}{2f_1} |\mathbf{p}| \Delta_{1,1} = \Pi(1, 0, 1, -1, 1), \quad (\text{B11})$$

$$\Pi(1, 1, 1, -1, 0) = -\frac{\lambda_2 \beta}{4\lambda_1 f_1} |\mathbf{p}| \Delta_{1,1} = \Pi(1, -1, 1, 1, 0), \quad (\text{B12})$$

$$\begin{aligned} \Pi(1, 1, 1, 0, -1) &= -\left(\frac{\lambda_2 f_2 \zeta}{8\lambda_1 f_1^2} + \frac{\sqrt{2}f_2}{8\lambda_1 f_1}\right) |\mathbf{p}| \Delta_{1,1} \\ &= \Pi(1, -1, 1, 0, 1), \end{aligned} \quad (\text{B13})$$

Here,

$$\lambda_1 = \frac{1}{2\alpha_\rho^2} + \frac{1}{8\alpha_\rho'^2} + \frac{3}{8\alpha_\lambda'^2} + \frac{R^2}{4}, \quad (\text{B14})$$

$$\lambda_2 = -\frac{\sqrt{3}}{4\alpha_\rho'^2} + \frac{\sqrt{3}}{4\alpha_\lambda'^2} - \frac{\sqrt{3}R^2}{6}, \quad (\text{B15})$$

$$\lambda_3 = \frac{1}{2\alpha_\lambda^2} + \frac{3}{8\alpha_\rho'^2} + \frac{1}{8\alpha_\lambda'^2} + \frac{R^2}{12}, \quad (\text{B16})$$

$$\lambda_4 = \frac{\sqrt{2}}{4\alpha_\rho'^2} + \frac{\sqrt{2}}{4\alpha_\lambda'^2} + \frac{R^2}{\sqrt{2}} \frac{m_2}{m_2 + m_5}, \quad (\text{B17})$$

$$\lambda_5 = -\frac{\sqrt{6}}{4\alpha_\rho'^2} + \frac{\sqrt{6}}{12\alpha_\lambda'^2} - \frac{R^2}{\sqrt{6}} \frac{m_2}{m_2 + m_5}, \quad (\text{B18})$$

$$\lambda_6 = \frac{1}{4\alpha_\rho'^2} + \frac{1}{12\alpha_\lambda'^2} + \frac{R^2}{2} \left(\frac{m_2}{m_2 + m_5} \right)^2, \quad (\text{B19})$$

$$f_1 = \lambda_3 - \frac{\lambda_2^2}{4\lambda_1}, \quad (\text{B20})$$

$$f_2 = \lambda_5 - \frac{\lambda_2\lambda_4}{2\lambda_1}, \quad (\text{B21})$$

$$f_3 = \lambda_6 - \frac{\lambda_4^2}{4\lambda_1}, \quad (\text{B22})$$

$$\varpi = \frac{\lambda_2 f_2}{4\lambda_1 f_1} - \frac{\lambda_4}{2\lambda_1}, \quad (\text{B23})$$

$$\zeta = \frac{1}{\sqrt{6}} + \frac{\lambda_2}{2\sqrt{2}\lambda_1}, \quad (\text{B24})$$

$$\beta = 1 + \frac{\varpi}{\sqrt{2}} + \frac{f_2}{2\sqrt{6}f_1}, \quad (\text{B25})$$

for the above expressions and

$$\begin{aligned} \Delta_{0,0} &= \left(\frac{1}{\pi\alpha_\rho'^2} \right)^{\frac{3}{4}} \left(\frac{1}{\pi\alpha_\lambda'^2} \right)^{\frac{3}{4}} \left(\frac{R^2}{\pi} \right)^{\frac{3}{4}} \left(\frac{\pi^2}{\lambda_1 f_1} \right)^{\frac{3}{2}} \\ &\times \exp \left[- \left(f_3 - \frac{f_2^2}{4f_1} \right) |\mathbf{p}|^2 \right] \\ &\times \left(-\sqrt{\frac{3}{4\pi}} \right) \left(\frac{1}{\pi\alpha_\rho'^2} \right)^{\frac{3}{4}} \left(\frac{1}{\pi\alpha_\lambda'^2} \right)^{\frac{3}{4}}, \end{aligned} \quad (\text{B26})$$

$$\begin{aligned} \Delta_{0,1} &= \left(\frac{1}{\pi\alpha_\rho'^2} \right)^{\frac{3}{4}} \left(\frac{1}{\pi\alpha_\lambda'^2} \right)^{\frac{3}{4}} \left(\frac{R^2}{\pi} \right)^{\frac{3}{4}} \left(\frac{\pi^2}{\lambda_1 f_1} \right)^{\frac{3}{2}} \\ &\times \exp \left[- \left(f_3 - \frac{f_2^2}{4f_1} \right) |\mathbf{p}|^2 \right] \\ &\times \frac{3i}{4\pi} \left(\frac{1}{\pi\alpha_\rho'^2} \right)^{\frac{3}{4}} \left(\frac{8}{3\sqrt{\pi}} \right)^{\frac{1}{2}} \left(\frac{1}{\alpha_\lambda'^2} \right)^{\frac{5}{4}}, \end{aligned} \quad (\text{B27})$$

$$\begin{aligned} \Delta_{1,0} &= \left(\frac{1}{\pi\alpha_\rho'^2} \right)^{\frac{3}{4}} \left(\frac{1}{\pi\alpha_\lambda'^2} \right)^{\frac{3}{4}} \left(\frac{R^2}{\pi} \right)^{\frac{3}{4}} \left(\frac{\pi^2}{\lambda_1 f_1} \right)^{\frac{3}{2}} \\ &\times \exp \left[- \left(f_3 - \frac{f_2^2}{4f_1} \right) |\mathbf{p}|^2 \right] \\ &\times \frac{3i}{4\pi} \left(\frac{8}{3\sqrt{\pi}} \right)^{\frac{1}{2}} \left(\frac{1}{\alpha_\rho'^2} \right)^{\frac{5}{4}} \left(\frac{1}{\pi\alpha_\lambda'^2} \right)^{\frac{3}{4}}, \end{aligned} \quad (\text{B28})$$

$$\begin{aligned} \Delta_{0,2} &= \left(\frac{1}{\pi\alpha_\rho'^2} \right)^{\frac{3}{4}} \left(\frac{1}{\pi\alpha_\lambda'^2} \right)^{\frac{3}{4}} \left(\frac{R^2}{\pi} \right)^{\frac{3}{4}} \left(\frac{\pi^2}{\lambda_1 f_1} \right)^{\frac{3}{2}} \\ &\times \exp \left[- \left(f_3 - \frac{f_2^2}{4f_1} \right) |\mathbf{p}|^2 \right] \\ &\times \frac{\sqrt{15}}{8\pi} \left(\frac{1}{\pi\alpha_\rho'^2} \right)^{\frac{3}{4}} \left(\frac{16}{15\sqrt{\pi}} \right)^{\frac{1}{2}} \left(\frac{1}{\alpha_\lambda'^2} \right)^{\frac{7}{4}}, \end{aligned} \quad (\text{B29})$$

$$\begin{aligned} \Delta_{2,0} &= \left(\frac{1}{\pi\alpha_\rho'^2} \right)^{\frac{3}{4}} \left(\frac{1}{\pi\alpha_\lambda'^2} \right)^{\frac{3}{4}} \left(\frac{R^2}{\pi} \right)^{\frac{3}{4}} \left(\frac{\pi^2}{\lambda_1 f_1} \right)^{\frac{3}{2}} \\ &\times \exp \left[- \left(f_3 - \frac{f_2^2}{4f_1} \right) |\mathbf{p}|^2 \right] \\ &\times \frac{\sqrt{15}}{8\pi} \left(\frac{16}{15\sqrt{\pi}} \right)^{\frac{1}{2}} \left(\frac{1}{\alpha_\rho'^2} \right)^{\frac{7}{4}} \left(\frac{1}{\pi\alpha_\lambda'^2} \right)^{\frac{3}{4}}, \end{aligned} \quad (\text{B30})$$

$$\begin{aligned} \Delta_{1,1} &= \left(\frac{1}{\pi\alpha_\rho'^2} \right)^{\frac{3}{4}} \left(\frac{1}{\pi\alpha_\lambda'^2} \right)^{\frac{3}{4}} \left(\frac{R^2}{\pi} \right)^{\frac{3}{4}} \left(\frac{\pi^2}{\lambda_1 f_1} \right)^{\frac{3}{2}} \\ &\times \exp \left[- \left(f_3 - \frac{f_2^2}{4f_1} \right) |\mathbf{p}|^2 \right] \\ &\times \left(-\frac{3}{4\pi} \right)^{\frac{3}{2}} \frac{8}{3\sqrt{\pi}} \left(\frac{1}{\alpha_\rho'^2 \alpha_\lambda'^2} \right)^{\frac{5}{4}}. \end{aligned} \quad (\text{B31})$$

Here, the parameters α_ρ' and α_λ' stand the harmonic oscillator parameters of the final singly heavy baryon.

- [1] M. Mattson *et al.* (SELEX Collaboration), First Observation of the Doubly Charmed Baryon Ξ_{cc}^+ , *Phys. Rev. Lett.* **89**, 112001 (2002).
 [2] M. A. Moinester *et al.* (SELEX Collaboration), First observation of doubly charmed baryons, *Czech. J. Phys.* **53**, B201 (2003).

- [3] R. Aaij *et al.* (LHCb Collaboration), Observation of the Doubly Charmed Baryon Ξ_{cc}^{++} , *Phys. Rev. Lett.* **119**, 112001 (2017).
 [4] H. X. Chen, Q. Mao, W. Chen, X. Liu, and S. L. Zhu, Establishing low-lying doubly charmed baryons, *Phys. Rev. D* **96**, 031501 (2017).

- [5] H. S. Li, L. Meng, Z. W. Liu, and S. L. Zhu, Magnetic moments of the doubly charmed and bottomed baryons, *Phys. Rev. D* **96**, 076011 (2017).
- [6] W. Wang, F. S. Yu, and Z. X. Zhao, Weak decays of doubly heavy baryons: The $1/2 \rightarrow 1/2$ case, *Eur. Phys. J. C* **77**, 781 (2017).
- [7] L. Meng, N. Li, and S. L. Zhu, Possible hadronic molecules composed of the doubly charmed baryon and nucleon, [arXiv:1707.03598](https://arxiv.org/abs/1707.03598).
- [8] W. Wang, Z. P. Xing, and J. Xu, Weak Decays of doubly heavy baryons: SU(3) analysis, *Eur. Phys. J. C* **77**, 800 (2017).
- [9] M. Karliner and J. L. Rosner, Discovery of Doubly-Charmed Xi_{cc} Baryon Implies a Stable ($bb\bar{u}\bar{d}$) Tetraquark, *Phys. Rev. Lett.* **119**, 202001 (2017).
- [10] E. J. Eichten and C. Quigg, Heavy-quark symmetry implies stable heavy tetraquark mesons $Q_i Q_j \bar{q}_k \bar{q}_l$, *Phys. Rev. Lett.* **119**, 202002 (2017).
- [11] T. Gutsche, M. A. Ivanov, J. G. Körner, and V. E. Lyubovitskij, Decay chain information on the newly discovered double charm baryon state Ξ_{cc}^{++} , *Phys. Rev. D* **96**, 054013 (2017).
- [12] F.-S. Yu, H.-Y. Jiang, R.-H. Li, C.-D. L. Wang, and Z.-X. Zhao, Discovery potentials of doubly charmed baryons, [arXiv:1703.09086](https://arxiv.org/abs/1703.09086).
- [13] J. Hu and T. Mehen, Chiral Lagrangian with heavy quark-diquark symmetry, *Phys. Rev. D* **73**, 054003 (2006).
- [14] R. Chen, A. Hosaka, and X. Liu, Prediction of triple-charm molecular pentaquarks, *Phys. Rev. D* **96**, 114030 (2017).
- [15] X. H. Hu, Y. L. Shen, W. Wang, and Z. X. Zhao, Weak decays of doubly heavy baryons: “decay constants”, [arXiv:1711.10289](https://arxiv.org/abs/1711.10289) [*Phys. Rev. D* (to be published)].
- [16] H. X. Chen, Q. Mao, W. Chen, X. Liu, and S. L. Zhu, Establishing low-lying doubly charmed baryons, *Phys. Rev. D* **96**, 031501 (2017).
- [17] L. Y. Xiao, K. L. Wang, Q. F. Lü, X. H. Zhong, and S. L. Zhu, Strong and radiative decays of the doubly charmed baryons, *Phys. Rev. D* **96**, 094005 (2017).
- [18] H.-S. Li, L. Meng, Z.-W. Liu, and S.-L. Zhu, Radiative decays of the doubly charmed baryons in chiral perturbation theory, *Phys. Lett. B* **777**, 169 (2018).
- [19] Q. F. Lü, K. L. Wang, L. Y. Xiao, and X. H. Zhong, Mass spectra and radiative transitions of doubly heavy baryons in a relativized quark model, *Phys. Rev. D* **96**, 114006 (2017).
- [20] D. Ebert, R. N. Faustov, V. O. Galkin, and A. P. Martynenko, Mass spectra of doubly heavy baryons in the relativistic quark model, *Phys. Rev. D* **66**, 014008 (2002).
- [21] R. Roncaglia, D. B. Lichtenberg, and E. Predazzi, Predicting the masses of baryons containing one or two heavy quarks, *Phys. Rev. D* **52**, 1722 (1995).
- [22] S. S. Gershtein, V. V. Kiselev, A. K. Likhoded, and A. I. Onishchenko, Spectroscopy of doubly heavy baryons, *Phys. Rev. D* **62**, 054021 (2000).
- [23] C. Itoh, T. Minamikawa, K. Miura, and T. Watanabe, Doubly charmed baryon masses and quark wave functions in baryons, *Phys. Rev. D* **61**, 057502 (2000).
- [24] W. Roberts and M. Pervin, Heavy baryons in a quark model, *Int. J. Mod. Phys. A* **23**, 2817 (2008).
- [25] T. Yoshida, E. Hiyama, A. Hosaka, M. Oka, and K. Sadato, Spectrum of heavy baryons in the quark model, *Phys. Rev. D* **92**, 114029 (2015).
- [26] Z. Shah, K. Thakkar, and A. K. Rai, Excited State Mass spectra of doubly heavy baryons Ω_{cc} , Ω_{bb} and Ω_{bc} , *Eur. Phys. J. C* **76**, 530 (2016).
- [27] S. S. Gershtein, V. V. Kiselev, A. K. Likhoded, and A. I. Onishchenko, Spectroscopy of doubly charmed baryons: Ξ_{cc}^+ and Ξ_{cc}^{++} , *Mod. Phys. Lett. A* **14**, 135 (1999).
- [28] J. R. Zhang and M. Q. Huang, Doubly heavy baryons in QCD sum rules, *Phys. Rev. D* **78**, 094007 (2008).
- [29] Z. G. Wang, Analysis of the $\frac{1}{2}^+$ doubly heavy baryon states with QCD sum rules, *Eur. Phys. J. A* **45**, 267 (2010).
- [30] Z. S. Brown, W. Detmold, S. Meinel, and K. Orginos, Charmed bottom baryon spectroscopy from lattice QCD, *Phys. Rev. D* **90**, 094507 (2014).
- [31] A. Faessler, T. Gutsche, M. A. Ivanov, J. G. Körner, and V. E. Lyubovitskij, Semileptonic decays of double heavy baryons, *Phys. Lett. B* **518**, 55 (2001).
- [32] C. Albertus, E. Hernandez, J. Nieves, and J. M. Verde-Velasco, Static properties and semileptonic decays of doubly heavy baryons in a nonrelativistic quark model, *Eur. Phys. J. A* **32**, 183 (2007); Erratum, *Eur. Phys. J. A* **36**, 119(E) (2008).
- [33] W. Roberts and M. Pervin, Hyperfine mixing and the semileptonic decays of double-heavy baryons in a quark model, *Int. J. Mod. Phys. A* **24**, 2401 (2009).
- [34] C. Albertus, E. Hernandez, and J. Nieves, Hyperfine mixing in $b \rightarrow c$ semileptonic decay of doubly heavy baryons, *Phys. Lett. B* **683**, 21 (2010).
- [35] A. Faessler, T. Gutsche, M. A. Ivanov, J. G. Körner, and V. E. Lyubovitskij, Semileptonic decays of double heavy baryons in a relativistic constituent three-quark model, *Phys. Rev. D* **80**, 034025 (2009).
- [36] A. I. Onishchenko, Exclusive decays of $\Xi_{QQ'}$ baryons in NRQCD sum rules, [arXiv:hep-ph/0006271](https://arxiv.org/abs/hep-ph/0006271).
- [37] V. V. Kiselev and A. K. Likhoded, Baryons with two heavy quarks, *Usp. Fiz. Nauk* **172**, 497 (2002) [*Phys. Usp.* **45**, 455 (2002)].
- [38] M. J. White and M. J. Savage, Semileptonic decay of baryons with two heavy quarks, *Phys. Lett. B* **271**, 410 (1991).
- [39] M. A. Sanchis-Lozano, Weak decays of doubly heavy hadrons, *Nucl. Phys.* **B440**, 251 (1995).
- [40] E. Hernandez, J. Nieves, and J. M. Verde-Velasco, Heavy quark symmetry constraints on semileptonic form-factors and decay widths of doubly heavy baryons, *Phys. Lett. B* **663**, 234 (2008).
- [41] X. H. Guo, H. Y. Jin, and X. Q. Li, Weak semileptonic decays of heavy baryons containing two heavy quarks, *Phys. Rev. D* **58**, 114007 (1998).
- [42] D. Ebert, R. N. Faustov, V. O. Galkin, and A. P. Martynenko, Semileptonic decays of doubly heavy baryons in the relativistic quark model, *Phys. Rev. D* **70**, 014018 (2004); Erratum, *Phys. Rev. D* **77**, 079903(E) (2008).
- [43] R. H. Hackman, N. G. Deshpande, D. A. Dicus, and V. L. Teplitz, M1 Transitions in the MIT Bag Model, *Phys. Rev. D* **18**, 2537 (1978).
- [44] T. Branz, A. Faessler, T. Gutsche, M. A. Ivanov, J. G. Körner, V. E. Lyubovitskij, and B. Oehl, Radiative decays of double heavy baryons in a relativistic constituent

- three-quark model including hyperfine mixing, *Phys. Rev. D* **81**, 114036 (2010).
- [45] A. Bernotas and V. Šimonis, Radiative M1 transitions of heavy baryons in the bag model, *Phys. Rev. D* **87**, 074016 (2013).
- [46] X. H. Zhong and Q. Zhao, Charmed baryon strong decays in a chiral quark model, *Phys. Rev. D* **77**, 074008 (2008).
- [47] S. Godfrey, Spectroscopy of B_c mesons in the relativized quark model, *Phys. Rev. D* **70**, 054017 (2004).
- [48] S. Godfrey and K. Moats, Bottomonium mesons and strategies for their observation, *Phys. Rev. D* **92**, 054034 (2015).
- [49] S. Godfrey and K. Moats, Properties of excited charm and charm-strange mesons, *Phys. Rev. D* **93**, 034035 (2016).
- [50] S. Godfrey, K. Moats, and E. S. Swanson, B and B_s meson spectroscopy, *Phys. Rev. D* **94**, 054025 (2016).
- [51] C. Chen, X. L. Chen, X. Liu, W. Z. Deng, and S. L. Zhu, Strong decays of charmed baryons, *Phys. Rev. D* **75**, 094017 (2007).
- [52] B. Chen and X. Liu, New Ω_c^0 baryons discovered by LHCb as the members of $1P$ and $2S$ states, *Phys. Rev. D* **96**, 094015 (2017).
- [53] Z. Zhao, D. D. Ye, and A. Zhang, Nature of charmed strange baryons $\Xi_c(3055)$ and $\Xi_c(3080)$, *Phys. Rev. D* **94**, 114020 (2016).
- [54] D. D. Ye, Z. Zhao, and A. Zhang, Study of $2S$ - and $1D$ - excitations of observed charmed strange baryons, *Phys. Rev. D* **96**, 114003 (2017).
- [55] D. D. Ye, Z. Zhao, and A. Zhang, Study of P -wave excitations of observed charmed strange baryons, *Phys. Rev. D* **96**, 114009 (2017).
- [56] L. Micu, Decay rates of meson resonances in a quark model, *Nucl. Phys.* **B10**, 521 (1969).
- [57] R. D. Carlitz and M. Kislinger, Regge amplitude arising from $su(6)_w$ vertices, *Phys. Rev. D* **2**, 336 (1970).
- [58] A. Le Yaouanc, L. Oliver, O. Pene, and J. C. Raynal, Naive quark pair creation model of strong interaction vertices, *Phys. Rev. D* **8**, 2223 (1973).
- [59] A. Le Yaouanc, L. Oliver, O. Pene, and J. C. Raynal, *Hadron Transitions in the Quark Model* (Gordon and Breach, New York, 1988), p. 311.
- [60] A. Le Yaouanc, L. Oliver, O. Pene, and J.-C. Raynal, Strong decays of ψ dblac; (4.028) as a radial excitation of charmonium, *Phys. Lett.* **71B**, 397 (1977); Why is $\psi(4.414)$ so narrow?, *Phys. Lett.* **72B**, 57 (1977).
- [61] C. Hayne and N. Isgur, Beyond the wave function at the origin: Some momentum dependent effects in the non-relativistic quark model, *Phys. Rev. D* **25**, 1944 (1982).
- [62] C. Patrignani *et al.* (Particle Data Group), Review of particle physics, *Chin. Phys. C* **40**, 100001 (2016).
- [63] N. A. Tornqvist and P. Zenczykowski, Ground state baryon mass splittings from unitarity, *Phys. Rev. D* **29**, 2139 (1984).
- [64] P. Geiger and N. Isgur, Strange hadronic loops of the proton: A quark model calculation, *Phys. Rev. D* **55**, 299 (1997).
- [65] Z. W. Liu, W. Kamleh, D. B. Leinweber, F. M. Stokes, A. W. Thomas, and J. J. Wu, Hamiltonian effective field theory study of the $N^*(1440)$ resonance in lattice QCD, *Phys. Rev. D* **95**, 034034 (2017).
- [66] H. García-Tecocoatzi, R. Bijker, J. Ferretti, and E. Santopinto, Self-energies of octet and decuplet baryons due to the coupling to the baryon-meson continuum, *Eur. Phys. J. A* **53**, 115 (2017).
- [67] J. F. Liu and G. J. Ding, Bottomonium Spectrum with coupled-channel effects, *Eur. Phys. J. C* **72**, 1981 (2012).
- [68] B. Q. Li, C. Meng, and K. T. Chao, Coupled-channel and screening effects in charmonium spectrum, *Phys. Rev. D* **80**, 014012 (2009).
- [69] J. Ferretti and E. Santopinto, Higher mass bottomonia, *Phys. Rev. D* **90**, 094022 (2014).
- [70] Y. Lu, M. N. Anwar, and B. S. Zou, Coupled-channel effects for the bottomonium with realistic wave functions, *Phys. Rev. D* **94**, 034021 (2016).
- [71] E. van Beveren and G. Rupp, Multichannel Calculation for D_s^* Vector States and the $D_{sJ}^+(2632)$ Resonance, *Phys. Rev. Lett.* **93**, 202001 (2004).